25-K phase transition in NpO_2 from ^{237}Np Mössbauer spectroscopy

J. M. Friedt and F. J. Litterst*
Centre de Recherches Nucléaires, 67037 Strasbourg Cedex, France

J. Rebizant
Commission of the European Communities, Joint Research Center, Karlsruhe Establishment, European Institute for Transuranium Elements, Postfach 2266, D-7500 Karlsruhe, Federal Republic of Germany

(Received 20 February 1985)

^{237}Np Mössbauer spectroscopy in magnetic external fields up to 8 T and in the temperature range 1.5—160 K, demonstrates that NpO_2 remains paramagnetic well below $T_c = 25$ K. The specific-heat anomaly, the cusp in magnetic susceptibility, and the changes in the shape of the Mössbauer spectra observed at 25 K are attributed to a structural transition. Both the bulk susceptibility and the Mössbauer data can be satisfactorily reproduced under the assumption of an inhomogeneous compressional-expansional internal distortion of the oxygen sublattice. It is suggested that a magnetic ordering of NpO_2 is prevented (or at least depressed) by this competitive structural transition.

I. INTRODUCTION

Despite considerable experimental and theoretical effort, the nature of the phase transition occurring at $T_c = 25$ K in cubic NpO_2 (CaF_2-type structure) has remained particularly puzzling: The temperature dependence of magnetic susceptibility $\chi(T)$ is characteristic for a Néel transition to an antiferromagnetic state.[1,2] On the other hand, ^{237}Np Mössbauer spectroscopy[3,4] and neutron elastic scattering[5–7] either unambiguously rule out such a magnetic ordering or indicate a fortuitous quenching of the $3.0\mu_B$ paramagnetic moment to an ordered moment of less than $0.2\mu_B$ or $0.01\mu_B$. The specific heat[8] and the lattice parameter[9] reveal anomalies in their temperature dependences at T_c. Some of these results, i.e., the susceptibility, and the specific-heat and lattice-parameter temperature dependences, are strongly reminiscent of those reported in the isostructural uranium oxyde UO_2, for which coinciding magnetic ordering and structural disordering of the oxygen sublattice are safely established at 30.8 K.[10,11]

On the other hand, the temperature dependence of $\chi(T)$ reported for AmO_2 is also in conflict with other results: The magnetic transition which would be established from $\chi(T)$ for the Am^{4+} (^8S) ion in AmO_2 (Ref. 12) contradicts the results from Mössbauer (Ref. 13) and neutron spectroscopy,[14] which rather safely rule out magnetic order.

Whereas much of the early discrepancies could conceivably be assigned to material problems related to stoichiometry and/or radiation-damage defects, recent studies have used high-quality single-crystal samples without solving these inconsistencies.

Accepting the tetravalent valence state Np^{4+} ($^4I_{9/2}$) in NpO_2 (which is clearly established from isomer-shift measurements and also supported by neutron scattering form factors),[7] the whole of the results gathered in NpO_2 with respect to the 25-K transition can be interpreted in terms of either an antiferromagnetic (or noncolinear) magnetic ordering, with a coincident quenching of the magnetic moment to a nearly zero value, or to a structural order-disorder transition of the oxygen sublattice, which would induce a singular temperature dependence of $\chi(T)$ below T_c via electronic rearrangement.[4,15]

The present work concerns new experimental developments of ^{237}Np Mössbauer spectroscopy in powdered polycrystalline or single-crystal samples of NpO_2, with the purpose of elucidating the phase transition occurring at T_c in this compound: local susceptibility measurements, accessible from external-magnetic-field Mössbauer spectroscopy at temperatures from 1.5 to 160 K, unambiguously characterize the paramagnetic nature of NpO_2 persisting well below $T_c = 25$ K.[4] The transition is assigned to an order-disorder transition of the oxygen sublattice, which would induce below T_c a splitting of the cubic crystal-field multiplets such as to reduce $\chi(T)$ on decreasing the temperature. A theoretical treatment of the crystal-field effects arising from the local-symmetry perturbation, similar to the one reported for UO_2,[10,11] allows a consistent representation for both the present new results and the previously published ones.

II. EXPERIMENTAL CONSIDERATIONS

For the present set of experiments, several samples of NpO_2 have been used, i.e., polycrystalline material or crushed single-crystal material of the same batch as used for the susceptibility measurements[2] and for the neutron-diffraction experiments.[7] (Note that the present single-crystal sample is from the same batch as the one reported in Ref. 4, but of slightly smaller thickness.) Structural and analytical considerations confirm the stoichiometry of the samples. For Mössbauer spectroscopy experiments, the samples were mounted in doubly encapsulated aluminum containers, sealed by electron-beam welding, with a uniform absorber superficial mass of 100 mg Np/cm^2 over a diameter of 13 mm. The absorber temperature is changed continuously from 1.5 to 300 K with a precision better than 0.5 K over the duration of a measurement by

using an anticryostat with regulated heating. The 100-mCi source of ^{241}Am metal is moved sinusoidally at 4.2 K (or 1.5 K). The absorber could be placed in an external magnetic field up to 8.5 T provided by a superconducting solenoid, at any temperature between 4.2 and 180 K. A compensation coil ensured zero fringing field at the level of the source; this is an essential aspect for the type of experiments considered since large broadenings are observed under magnetic field for Np impurities diluted in Am metal probably via a Kondo mechanism.[16] For detection of the 59.6-keV γ radiation we used an intrinsic Ge diode.

The data are computer fitted to either single-line, quadrupole, or magnetic hyperfine interactions. In the latter case, the spectral line shape is calculated with no approximation (except for intensity saturation effects due to finite absorber thickness), by calculating the transition energies and intensities after diagonalization of the nuclear hyperfine matrices, including an anisotropic magnetic hyperfine interaction for the external-field data below T_c (see below). The result is convoluted with a Lorentzian line shape modified by a dispersion term for each individual component, the full width at half maximum (FWHM) being taken to the constant value measured above T_c ($W=2.93\pm0.03$ mm/s), which also is close to the minimum measured value. The broadening of the measured W in comparison to the theoretical value is assigned to the result of radiation-damage effects in the source material.[4] The validity of such a broadened Lorentzian line shape is consistently established from many earlier studies; in particular, from investigations of absorber materials presenting resolved quadrupole or magnetic hyperfine splittings.[4] The dispersion modification of the Lorentzian line shape arises from the interference between nuclear absorption followed by internal conversion and photoelectric absorption, which is large for an $E1$ Mössbauer transition;[17] the dispersion term of the resulting line shape,

$$R(v) \propto \left[1-2\xi\frac{E_\gamma v/c}{W/2}\right]\left[1+\left[\frac{E_\gamma v/c}{W/2}\right]^2\right]^{-1}$$

(E_γ is the transition energy, v the relative Doppler velocity between source and absorber, c the velocity of light, and the resonance occurs at $v=0$), is found experimentally to be $2\xi=0.055$, in agreement with theoretical estimate.

III. EXPERIMENTAL RESULTS

Zero-external-field measurements above T_c, from 26 to 200 K, are well represented by a single, dispersion-corrected, Lorentzian absorption, for both single-crystal and polycrystalline powder samples (Fig. 1). The single-line width W_{SL} changes from 2.70 ± 0.03 to 2.93 ± 0.03 mm/s from 200 to 26 K (Fig. 2), due primarily to effective-absorber-thickness ($n\sigma_0 f_A$) changes via change of the recoil-free fraction (n is the number of resonant atoms per unit surface, σ_0, the absorption cross section, and f_A the absorber recoil-free fraction). The isomer shift ($\delta_{IS}=7.70\pm0.05$ mm/s against Am metal) is clearly characteristic for the Np^{4+} valence configuration.

Zero-field data below T_c essentially reveal a sudden broadening of the single absorption line (Figs. 1 and 2).

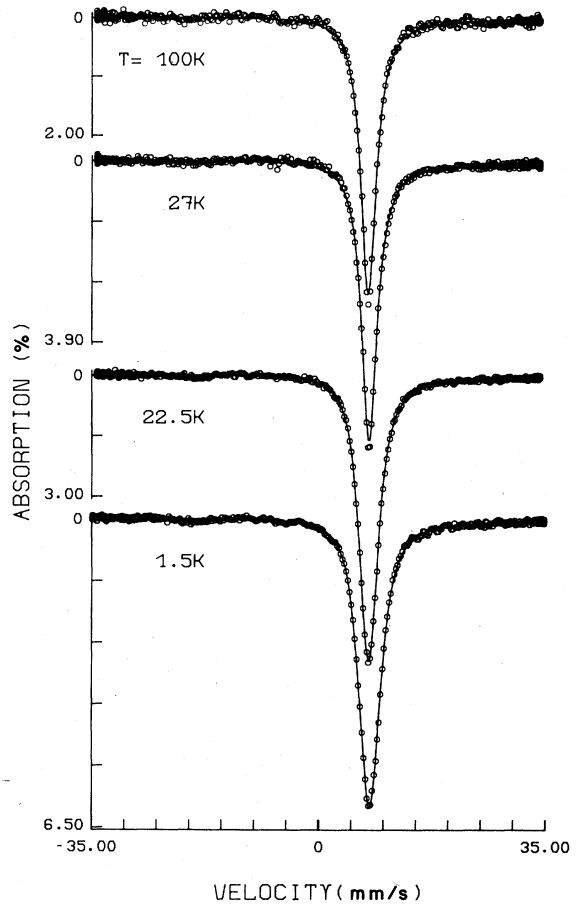

FIG. 1. Temperature dependence of the ^{237}Np Mössbauer spectra of crushed single-crystal $NpO_{2.00}$. The solid lines represent the result of computer fits, i.e., single resonance line above $T_c=25$ K and quadrupole splitting below T_c.

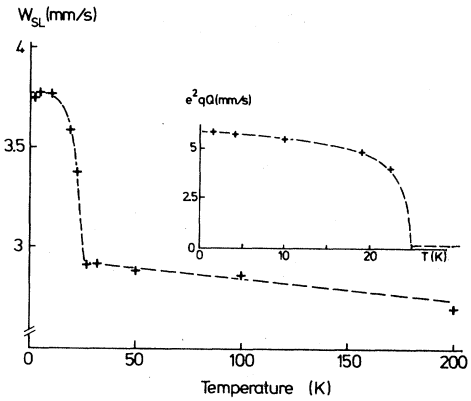

FIG. 2. Temperature dependence of the pseudolinewidth (W_{SL}) when assuming a single-line fit over the whole temperature range for a powdered single crystal of NpO_2. Inset: Temperature dependence of the quadrupole coupling constant e^2qQ determined from zero-field measurements (Fig. 1). The dotted lines serve merely as a guide to the eye.

Similar to earlier reports,[3,4] the broadening is found to be sample dependent, without detectable correlation to any physical or chemical parameters of the compound. These data are perfectly represented in terms of a mere quadrupole splitting of the $\frac{5}{2}^+$ and $\frac{5}{2}^-$ nuclear levels, yielding, of course, slightly different quadrupole coupling constants for the different samples (Figs. 1 and 2). The powdered single-crystal sample NpO_2 can be considered as the most reliable material for representing the intrinsic properties: For this sample, a quadrupole coupling constant of $e^2qQ = 5.1 \pm 0.2$ mm/s (236 MHz) is deduced at 4.2 K. The onset of a magnetic hyperfine splitting, with an effective field (B_{hf}) of only 4.6 T at 4.2 K (Refs. 3 and 4) and no quadrupole interaction, cannot be definitely ruled out, although yielding a slightly worse quality of fit.

External-magnetic-field (B) data above T_c, up to 180 K, are well analyzed in terms of an effective field (B_{eff}) acting at the Np^{4+} nucleus with the nuclear spin polarized along the external field direction (in our geometry, parallel to the γ-ray direction) (Fig. 3). This allows the measurement of a local magnetic susceptibility B_{eff}/B, whose temperature dependence is found to follow closely the bulk magnetic susceptibility.

Several interpretations may be considered for the external-field results below T_c: Bulk antiferromagnetism would result in a superposition of two magnetic subspectra with effective fields $B_{hf} \pm B$ and polarization of the electronic moment along the external field (or perpendicular in the hypothesis of a metamagnetic transition). Data analysis along such a model unambiguously delivers inconsistent results as far as the values obtained for B_{eff} in the several B at various temperatures T are concerned. A canted spin magnetic ordering would deliver essentially similar results. In the situation of a spin-glass state, the spectra would essentially be unchanged by an external field, contrary to experiment.

On the other hand, a very good representation of the whole of the experimental results (Fig. 3) is achieved under the assumption of a quadrupole splitting occurring below T_c, with a random orientation between the electric-field-gradient (EFG) principal axis and the effective field, B_{eff}, being anisotropic as predicted from an electronic model discussed below [$B_{eff} = B + B_{hf}(\theta)$, where θ represents the orientation of B with respect to the crystalline-electric-field (CEF) axes and B_{hf} depends on this angle below T_c]. The electronic model discussed in Sec. IV predicts the appearance of two sets of EFG's of equal intensity with opposite sign and a nearly equal modulus below T_c. The anisotropic magnetic moment $\mu_Z(\theta)$ is calculated from this model and allows calculation of the anisotropic $B_{hf}(\theta)$. Very good and consistent agreement is indeed achieved by using this model of hyperfine interactions, despite the small number of free parameters (Fig. 3).

In summary, the present external-magnetic-field results unambiguously rule out the occurrence of collective magnetic order below T_c; on the other hand, a very good representation of the results is reached by assuming a structural transition occurring at T_c. This induces the appearance of an EFG at the Np nuclei below T_c. The low-temperature results in external magnetic field

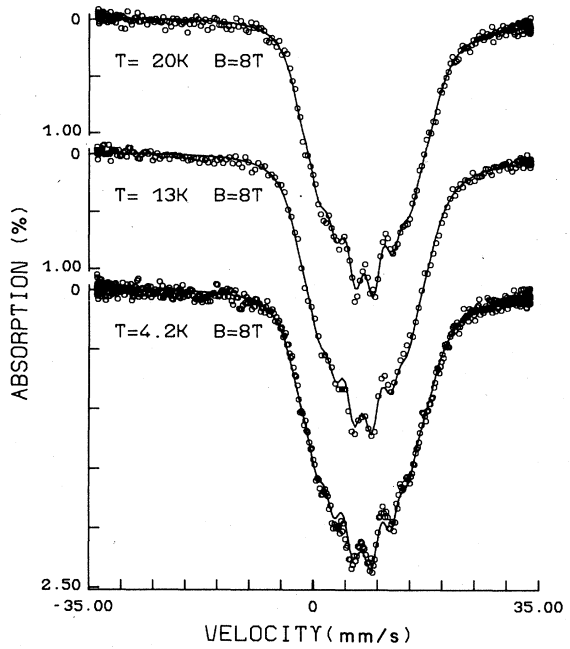

FIG. 3. ^{237}Np Mössbauer spectra of $NpO_{2.00}$ in an applied magnetic field at various temperatures. The solid lines correspond to computer fits, i.e., a simple effective-field situation above $T_c = 25$ K; below T_c, spectra are calculated for two quadrupole interactions with anisotropic B_{hf} and random orientation of the quantization axis with respect to the applied magnetic field (see text).

($T < T_c$) correspond to a paramagnetic situation with an anisotropic B_{eff}. The model description for this analysis is described in the next section.

IV. STRUCTURAL AND ELECTRONIC MODEL FOR THE PHASE TRANSITION

The primary aim of this section is to provide a consistent description for the whole of the experimental results available on the phase transition under consideration. Since external-magnetic-field Mössbauer spectroscopy data definitely rule out the presence of an ordered moment below T_c, a model must be searched for that explains the decrease of susceptibility, $\chi(T)$ (Refs. 1 and 2), below this temperature. This is found readily in terms of a structural transition, causing a lowering of the symmetry at the Np site, as indicated by the appearance of an EFG below T_c. There is no evidence for this transition from neutron scattering[5,6] and x-ray diffraction (except for a slight decrease of the lattice parameter at T_c).[9] This suggests the occurrence of an order-disorder transition of the oxygen sublattice only, similar to the one which is well established in UO_2 (nevertheless, in this compound, an internal shear transition of the oxygen sublattice coincides with an antiferromagnetic ordering).[10,11,18,19]

A crystal-field model is developed hereafter in order to represent the susceptibility and Mössbauer spectroscopy results, similar to the elastic distortion model established for UO_2. At temperature $T > T_c$, the CEF set up by the eightfold cubic O^{2-} coordination at the Np site is described by the usual Hamiltonian (axis of quantization: [001]):

$$\mathcal{H}_C = B_4^0 \beta_J \langle r^4 \rangle (O_4^0 + 5O_4^4) + B_6^0 \gamma_J \langle r^6 \rangle (O_6^0 - 21O_6^4) , \quad (1)$$

where the $\langle r^n \rangle$ are radial moments of the $5f$-electron charge distribution, and α_J (used later), β_J, γ_J, and O_n^m are Stevens reduced matrix elements and operator equivalents, respectively, within a given total-angular-momentum J multiplet.[20] Possible J mixing effects or deviations from the Russell-Saunders coupling scheme were checked to be negligible as far as concerning the lowest CEF level structure which, alone, is relevant for the considered properties. The ratio of the CEF parameters B_4^0/B_6^0 is derived from the value known in UO_2: $x_{UO_2} = 0.9$ and yields $x_{NpO_2} = -0.74$.[20,21] The modulus for $B_4^0\langle r^4 \rangle$ is selected as 1600 K from an analysis of the high-temperature $\chi(T)$ data. Although this procedure is known to be of limited sensitivity, it is applied in the absence of a direct measurement of CEF splittings within the ground multiplet. Nevertheless, the estimate is acceptable when considering that it is intermediate between extrapolations from the measured CEF splitting in PrO_2 (which yields $B_4^0\langle r^4 \rangle \simeq 1300$ K),[22] from optical data on Np^{4+} in ThO_2 (~ 800 K),[23] and from scaling of the value of UO_2 (~ 5400 K).[21] With the above parameters, Eq. (1) provides a ground-state $\Gamma_8^{(2)}$ quartet, followed by a $\Gamma_8^{(1)}$ quartet at 1000 K and a Γ_6 doublet at 2600 K. The single-ion magnetic susceptibility χ_0 is calculated by including a Zeeman perturbation,

$$\mathcal{H}_Z = -\mathbf{B} \cdot \mathbf{J}_Z g_J \beta_e , \quad (2)$$

($\mathbf{B}$ is the applied magnetic field, g_J the Landé factor, and β_e the Bohr magneton), and by considering both the direct and Van Vleck contributions. The measured Curie-Weiss behavior[2] is well represented in the molecular-field approximation:

$$\chi = \frac{\chi_0}{1 + \chi_0 C} , \quad (3)$$

with a value for $C \simeq 90 \pm 5$ mol/emu, corresponding to a Curie-Weiss temperature of -150 ± 10 K. The proposed set of parameters allows an excellent representation of the experimental temperature dependence of $\chi(T)$ above T_c [Fig. 4(a)]. It is worth noting that $\chi(T)$ and the normalized hyperfine fields measured from Mössbauer spectroscopy in an external field above T_c,

$$\frac{B_{hf}}{B} = \frac{B_{eff} - B}{B} , \quad (4)$$

are in good agreement when scaled linearly [Fig. 4(a)]. This is indeed predicted from the linear relationship between $\langle J_Z \rangle$ and both the orbital and core polarization contributions to B_{hf}.[24] An extrapolation of the B_{hf} to the free-ion value ($\langle J_Z \rangle = \frac{9}{2}$) yields a value $B_{hf}(FI) = 690 \pm 50$ T, which compares reasonably well with the earlier estimate of 590 T. The latter value would be reached under the assumption that the experimental absolute $\chi(T)$ values were too low by $\sim 10\%$. On the other hand, the accepted free-ion value (590 T) also suffers from uncertainty since, on one hand, it depends on calculated electronic parameters, or, alternatively, relies on the extrapolation of only a few experimental data points.[24] The whole of the result

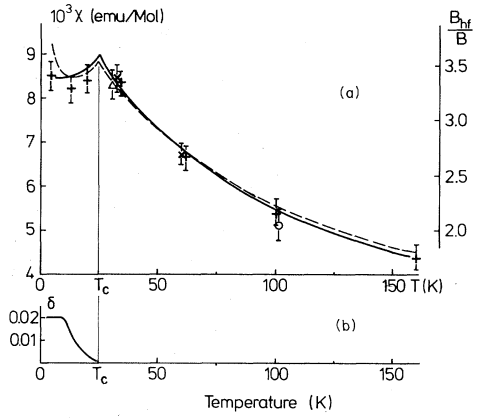

FIG. 4. (a) Experimental $\chi(T)$ (Ref. 2) (solid line) and calculated susceptibility (dashed line) [the electromagnetic units, left-hand scale, are used for direct comparison with the experiment (Ref. 2)]. The data symbols represent the normalized hyperfine fields B_{hf}/B (right-hand scale) which are derived from the Mössbauer data in several external fields (indicated by different symbols). Below $T_c = 25$ K, the angular averaged B_{hf} are represented. (b) Distortional parameter δ (see text) chosen for best agreement between model calculated and experimental $\chi(T)$ below $T_c = 25$ K.

indicates that the measured $\chi(T)$ arises entirely from the Np^{4+} contribution; in particular, a conceivable contribution from paramagnetic defects is ruled out since this would even further enhance the evaluated $B_{hf}(FI)$ and, moreover, destroy the linear relationship between $\chi(T)$ and B_{hf}/B.

Below the transition temperature T_c, we assume an internal distortion of the oxygen sublattice with the Np^{4+} ions staying paramagnetic. The resulting local-symmetry reduction induces an anisotropic magnetic moment (in comparison to the isotropic situation occurring at $T > T_c$), which leads to a reduced average moment of the powder sample and hence accounts for the decrease of $\chi(T)$ below T_c. The choice between the conceivable distortions (e.g., the homogeneous "Allen" shear mode[18] or inhomogeneous combinations of normal modes[19]) is dictated by the Mössbauer spectroscopy results, which definitely rule out *extreme* anisotropy of the resulting ground multiplet. Indeed, the spectra in an external field are relatively close to an "effective" field pattern, whereas extreme anisotropy of the magnetic moment (e.g., $\mu_\perp \simeq 0$) would cause a wider distribution of B_{eff} than observed experimentally. These considerations rule out distortions which would split the $\Gamma_8^{(2)}$ ground multiplet into extremely anisotropic Kramers doublets.

A consistent description for both the Mössbauer and $\chi(T)$ results is found under assumption of a longitudinal $A_{1g} + E_g$ distortion mode of the oxygen sublattice (Fig. 5). This involves a compression of one-half of the oxygen coordination units and an equal expansion of the other half.

The proposed mechanism involves a perturbation of the cubic CEF Hamiltonian [Eq. (1)], which is evaluated to second order as a function of the displacement of the oxygen sublattice $\delta = \Delta a/a$ (a is the cubic lattice constant) with a point-charge model as

$$\mathcal{H}_p=\frac{8Ze^2}{3d^3}\alpha_J\langle r^2\rangle\rho(\delta-\tfrac{7}{6}\delta^2)O_2^0+\frac{Ze^2}{9d^5}\beta_J\rho\langle r^4\rangle[(\tfrac{5}{2}\delta+10\delta^2)O_4^0+(\tfrac{105}{2}\delta-70\delta^2)O_4^4]$$
$$+\frac{Ze^2}{54d^7}\gamma_J\langle r^6\rangle\rho[(-35\delta+77\delta^2)O_6^0+(231\delta-77\delta^2)O_6^4]\ . \quad (5)$$

The effective charges Ze of the oxygen atoms are at a distance d from the Np^4 ions. The fourth- and sixth-order prefactors are readily substituted by using the above-used values:

$$B_4^0=-\frac{7}{18}\frac{Ze^2}{d^5},\quad B_6^0=\frac{1}{9}\frac{Ze^2}{d^7}\ .$$

A value of 18 300 K is used for the term $Ze^2\langle r^2\rangle/d^3$, which corresponds to unscreened oxygen charges at a distance $d=2.34$ Å. The parameter ρ represents an enhancement of the distortional term by reference to the mere point-charge model[19] and is taken as $\rho=10$ for both compressional and elongational distortions. One may note that all uncertainties with respect to the value of ρ can equivalently be represented by a different choice of effective charges or distortion amplitudes.

Using the extended CEF Hamiltonian [Eq. (5)], the susceptibilities are calculated along different crystal-lattice reference directions. The bulk susceptibility is calculated from averaging over all directions of the distortion axis and for both modes, including the molecular-field parameter C determined from χ above T_c. For obtaining reasonable agreement with the experimental susceptibilities,[2] we have to assume that δ increases *continuously* below T_c up to about $\delta=0.02$ below 10 K (Fig. 4). This conclusion is also consistent with the Mössbauer spectroscopic results, which reveal a rather progressive increase of e^2qQ below T_c.

Notably, the calculations predict a rapid increase of $\chi_c(T)$ at low temperature, even in case of a further increase of δ. This is expected since one is dealing with a Kramers ion. At the lowest reported temperature of $\chi(T)$ measurements (5 K),[2] however, only a leveling off is apparent. Apart from this deviation at lowest temperatures, the model calculation accounts satisfactorily for the measured $\chi(T)$.

The Mössbauer spectra in an external field are equally well represented (Fig. 3) by the model when considering the anisotropic magnetic moment, i.e., the predicted distribution of B_{hf}. The *distortion* was assumed to *vary slowly* on the timescale of the hyperfine-interaction measurement ($\sim10^{-8}$ s), i.e., the quadrupole interaction is not averaged out to zero. The *magnetic relaxation* is found to *be fast,* i.e., B_{hf} represents a thermal average over the lowest-lying CEF levels, such that $B_{hf}\propto\langle J_Z\rangle$. This is a reasonable mechanism in view of the composition of the ground-multiplet wave functions including components $|J_Z\pm1\rangle$. Tentative fits including magnetic fluctuations of intermediate rate below T_c improved the quality of the analysis only slightly, yielding rates at the upper limit of possible detection ($\simeq5\times10^{12}$ s^{-1}). The EFG's at the Np^{4+} ions in both the elongated and compressed coordination units are found to be of axial symmetry (in agreement with the CEF distortion); the resulting sites present e^2qQ values (4 to 6 mm/s) of opposite signs and nearly equal moduli, which also coincide with those deduced in the absence of external field.

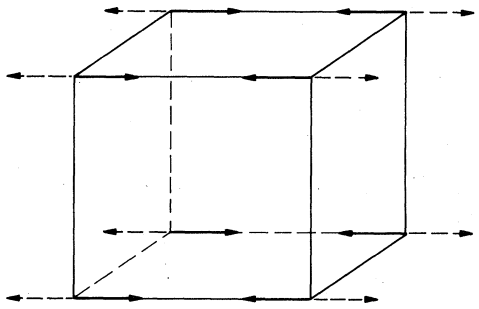

FIG. 5. Structural distortion (elongation-compression) proposed for the oxygen sublattice of NpO_2 below T_c.

The CEF calculations predict positive and negative contributions to the EFG's from the distorted $5f$-electronic shell for the expanded and compressed coordination units, respectively. Data analysis rather favors an opposite assignment. This may conceivably arise from the lattice contribution provided by the oxygen point charges, which is of opposite sign and may dominate the $5f$ contribution. A direct estimate for the respective contributions reveals a dominant lattice effect for $\delta>0.005$ when taking the reasonable values of $(1-\gamma_\infty)=100$ for the Sternheimer antishielding factor and $\rho=10$.

In Fig. 4(a) are also included the normalized hyperfine fields [Eq. (4)] for $T<25$ K. For a comparison between the macroscopic $\chi(T)$ and this microscopic susceptibility, we used the angular averaged B_{hf}. Good agreement between bulk and Mössbauer data is hence observed both above and below T_c within experimental error.

In summary, the proposed model of an elongation-compression structural disorder of the oxygen sublattice in NpO_2 provides a quantitative representation for both the bulk susceptibility and local external-magnetic-field Mössbauer spectroscopy results, at least down to ~10 K. The predicted increase of $\chi(T)$ below ~8 K requires experimental testing; actually, our lowest-temperature Mössbauer results (4.2 K) in field and the lowest-temperature $\chi(T)$ data (5 K) indicate a leveling off of the decreasing susceptibility as temperature decreases. Consistent with the neutron-diffraction results, no *ordered* magnetic moment occurs certainly down to 5 K and likely down to 1.5 K [from the present zero-field Mössbauer results (Figs. 1 and 2)]. The broad peak in specific heat, the smooth increase of the EFG's below a sharply defined T_c, and the smooth decrease of $\chi(T)$ below T_c suggest a second-order nature of the structural phase transition. It may be noted that the slight decrease of the lattice constant below 25 K cannot be explained in the frame of the proposed model. On the other hand (although impossible to interpret in the absence of understanding of the

broadening of the ^{237}Np resonance above T_c and because of the large absorber thickness in comparison to theory), the anomaly observed for the resonance intensity[4] is rather characteristic for a change of the phonon modes at T_c. Clearly, the reported experimental results concerning the phase transition in NpO_2 cannot provide a direct unambiguous proof for the proposed mechanism. This would involve elastic constant measurements or local-symmetry information as available from Raman and infrared spectroscopy.

The absence of magnetic ordering in NpO_2 as compared to UO_2 is not understood precisely. However, the different electronic ground-state structures and the different structural disordering of the oxygen sublattice may account for the different magnetic behaviors. As pointed out in the calculations for UO_2,[18] a strong enough structural distortion may suppress the onset of magnetic order. However, a self-consistent treatment of the counterplay of elastic, magnetoelastic, and magnetic energies seems impossible at this stage since elastic data are not available. In this context it is of interest to note the report of magnetic order in the $(Np_xU_{1-x})O_2$ solid solution, with reasonably large saturation hyperfine fields at the Np^{4+} site (100–120 T).[25] However, the mechanism of ordering may be complicated in these solid solutions because of the combined frustration of the structural disorder and of magnetism. The reported absence of magnetic hyperfine interaction for very dilute ^{237}Np atoms in the UO_2 host[26] is considered as nonsignificant since the radiation damage preceding the formation of the Np atom by nuclear reaction may likely disturb the magnetic superexchange paths via atomic disorder and bond rupture. We have found similar inconsistent results in a Mössbauer emission spectroscopy study of ^{237}Np formed by α decay of ^{241}Am diluted in UO_2 (3%), which failed to reveal magnetism down to 4.2 K, again because of the disruptive consequences of the recoil effects.[4]

V. SUMMARY AND CONCLUSIONS

The presented Mössbauer data in applied magnetic field reveal that NpO_2 remains paramagnetic well below $T_c = 25$ K, in agreement with neutron-scattering results. The anomaly in specific heat, the cusp in magnetic susceptibility, and changes in the shape of the Mössbauer spectra are assigned to a structural transition at this temperature. Similar to the case of UO_2, an inhomogeneous internal distortion of the oxygen sublattice is invoked in NpO_2: In contrast to the combined shear and rotational mode demonstrated for UO_2,[10] a compressional-expansional mode provides better agreement with experiment. Both bulk susceptibility and Mössbauer data are reproduced quantitatively using a simple crystal-field model. However, the model predicts an increase of the susceptibility below ~ 8 K, whereas the experimental data rather reveal a leveling off.

It is proposed that NpO_2 represents a system with competition between magnetic interactions and cooperative distortional forces. In contrast to UO_2 the magnetic interaction is overwhelmed (at least down to ~ 1.5 K) by the gain in energy due to the distortion of the oxygen sublattice. Whether the structural transition is driven by a Jahn-Teller effect (lifting the degeneracy of the $\Gamma_8^{(2)}$ ground state) or by an ordering of the Np^{4+} ion quadrupoles cannot be decided. In particular, low-temperature elastic constants would be necessary for an unequivocal assignment of the distortion.

ACKNOWLEDGMENTS

The skillful technical help of R. Poinsot is gratefully acknowledged. We thank J. C. Spirlet for the preparation of the NpO_2 single-crystal samples.

*On leave of absence from the Technische Universität, München.

[1] J. W. Ross and D. J. Lam, J. Appl. Phys. **38**, 1451 (1967).
[2] P. Erdös, G. Solt, Z. Zołnierek, A. Blaise, and J. M. Fournier, Physica **102B**, 164 (1980).
[3] B. D. Dunlap, G. M. Kalvius, D. J. Lam, and M. B. Brodsky, J. Phys. Chem. Solids **29**, 1365 (1968).
[4] J. M. Friedt, Radiochim. Acta **32**, 105 (1983).
[5] A. Boeuf, R. Caciuffo, J. M. Fournier, L. Manes, J. Rebizant, F. Rustichelli, J. C. Spirlet, and A. Wright, Phys. Status Solidi A **79**, K1 (1983).
[6] A. Boeuf, J. M. Fournier, G. Heger, N. Lehner, L. Manes, J. Rebizant, F. Rustichelli, and J. C. Spirlet, J. Phys. (Paris) Lett. **42**, L401 (1981).
[7] A. Delapalme, M. Forte, J. M. Fournier, J. Rebizant, and J. C. Spirlet, Physica **102B**, 171 (1980).
[8] E. F. Westrum, J. B. Hatcher, and D. W. Osborne, J. Chem. Phys. **21**, 419 (1953).
[9] J. A. C. Marples, in *Plutonium 1975 and other Actinides,* edited by H. Blank and R. Lindner (North-Holland, Amsterdam, 1976), p. 357.
[10] J. Faber and G. H. Lander, Phys.Rev. B **14**, 1151 (1976).
[11] J. Faber, G. H. Lander, and B. R. Cooper, Phys. Rev. Lett. **35**, 1770 (1975).
[12] D. G. Karraker, J. Chem. Phys. **63**, 3174 (1975).
[13] J. M. Friedt, J. Rebizant, R. Poinsot, and W. Muller, J. Phys. (Paris) Colloq. **37**, C6-935 (1976).
[14] A. Boeuf, J. M. Fournier, J. F. Guegnon, L. Manes, J. Rebizant, and F. Rustichelli, J. Phys. (Paris) Lett. **40**, L335 (1979).
[15] A. Zołnierek, G. Solt, and P. Erdös, J. Phys. Chem. Solids **42**, 773 (1981).
[16] J. M Friedt (unpublished); B. D. Dunlap, M. B. Brodsky, G. M. Kalvius, and G. K. Shenoy, in *Plutonium 1970,* edited by W. N. Miner (Metallurgical Society of AIME, New York, 1971), p. 331.
[17] G. T. Trammel and J. P. Hannon, Phys. Rev. **180**, 337 (1969).
[18] S. J. Allen, Phys. Rev. **167**, 492 (1968).
[19] R. Siemann and B. R. Cooper, Phys. Rev. B **19**, 2645 (1979); **20**, 2869 (1979).
[20] K. R. Lea, M. J. M. Leask, and W. P. Wolf, J. Phys. Chem. Solids **23**, 1381 (1962).
[21] H. U. Rahman and W. A. Runciman, J. Phys. Chem. Solids **27**, 1833 (1966).

[22]S. Kern, C. K. Loong, J Faber, and G. H. Lander, Solid State Commun. **49**, 295 (1984).
[23]J. B. Gruber and E. R. Menzel, J. Chem. Phys. **50**, 3772 (1969).
[24]B. D. Dunlap and G. H. Lander, Phys. Rev. Lett. **33**, 1046 (1974); B. D. Dunlap and G. M. Kalvius, Int. J. Magn. **2**, 231 (1972).
[25]A. Tabuteau, J. Jove, M. Pages, C. H. De Novion, and J. Gal, Solid State Commun. **50**, 357 (1984).
[26]R. D. Meeker, B. D. Dunlap, and D. Cohen, J. Phys. Chem. Solids **37**, 551 (1976).